Japanese Journal of Applied Physics
Vol. 47, No. 7, 2008, pp. 6088–6091

A Scanning Tunneling Microscopy Observation of ($\sqrt{3} \times \sqrt{3}$) R30° Reconstructed $Ni_2P(0001)$

Kumiko KINOSHITA[1,2], Georg Hermann SIMON[3], Thomas KÖNIG[3], Markus HEYDE[3], Hans-Joachim FREUND[3], Yuta NAKAGAWA[1,2], Shushi SUZUKI[1,2,4], Wang-Jae CHUN[4,5], Shigeo Ted OYAMA[6], Shigeki OTANI[7], and Kiyotaka ASAKURA[1,2*]

[1]*Section of Surface Structure Chemistry and Research Cluster of Well-defined Surface Materials, Catalysis Research Center, Hokkaido University, Sapporo 001-0021, Japan*
[2]*Department of Quantum Science and Technology, Hokkaido University, Sapporo 060-8628, Japan*
[3]*Fritz-Haber-Institute of the Max-Planck-Society, D-14195 Berlin, Germany*
[4]*CREST-JST, Kawaguchi, Saitama 332-0012, Japan*
[5]*Division of Natural Sciences, International Christian University, Mitaka, Tokyo 181-8585, Japan*
[6]*Department of Chemical Engineering, Virginia Polytechnic Institute and State University, Blacksburg, VA 24061, U.S.A.*
[7]*National Institute for Material Science, Tsukuba, Ibaraki 305-0044, Japan*

(Received January 15, 2008; accepted February 21, 2008; published online July 18, 2008)

A $Ni_2P(0001)$ single crystal surface has been studied in the framework of model catalysis with a low temperature scanning tunneling microscope (STM) under ultrahigh vacuum (UHV). We observed a previously unreported ($\sqrt{3} \times \sqrt{3}$) R30° reconstruction and successfully recorded its atomically-resolved STM images. Two types of atomic arrangements have been found for this ($\sqrt{3} \times \sqrt{3}$) R30° structure depending on annealing conditions during preparation. One shows a filled and the other one an empty network of polygons. Upon annealing to 940 K, only the latter empty type of structure has been observed. [DOI: 10.1143/JJAP.47.6088]

KEYWORDS: $Ni_2P(0001)$ surface, Ni_3P-terminated surface, Ni_3P_2-terminated surface, ($\sqrt{3} \times \sqrt{3}$) R30° reconstruction, STM

1. Introduction

New environmental regulations for reducing motor vehicle emissions have led to a worldwide search for new hydrotreating catalysts for removing sulfur from petroleum feedstocks by hydrodesulfurization (HDS). Among alternatives to the widely used sulfides next generation catalysts are transition-metal phosphides,[1–3] a group of refractory metallic compounds with excellent activity for HDS.[1–9] A review of the subject indicates that Ni_2P is the most active of the phosphides.[10]

To understand the structural and energetic origin of such high activity, detailed atomic scale surface science studies are desirable. So far a foundation has been laid with works on $Ni_2P(0001)$ single crystal surfaces. Low energy electron diffraction (LEED), X-ray photoelectron spectroscopy (XPS), and scanning tunneling microscopy (STM) studies have been carried out.[11–13] Structural and adsorption properties of $Ni_2P(0001)$ have been studied by the density functional theory (DFT) method.[14,15] Most of these works focus on a (1 × 1) unreconstructed surface. On the other hand the wealth of compounds between Ni and P such as Ni_3P, Ni_8P_3, Ni_5P_2, $Ni_{12}P_5$, Ni_2P, Ni_5P_4, NiP, NiP_2, and NiP_3[16,17] suggest that structures different from (1 × 1) can be created on the surface depending on surface composition. We have observed a new ($\sqrt{3} \times \sqrt{3}$) R30° reconstructed structure that varies between two related appearances with raising preparation temperature. In this paper we show STM results from these reconstructed surfaces.

2. Experimantal Methods

All experiments have been carried out in an UHV system ($\sim 10^{-8}$ Pa), equipped with an Argon ion gun, a four-grid reverse view LEED optics (SPECS ErLEED100) and a quadrupole mass spectrometer (Pfeiffer Vacuum Prisma QMS200). Further details on the custom-built STM setup, located at the Fritz-Haber Institute of the Max-Planck Society in Berlin, can be found elsewhere.[18,19] While LEED images have been recorded at room temperature, all STM images have been obtained at low temperature (4–5 K) in a constant current mode. A cut Pt–Ir wire has been used as a STM probe. The $Ni_2P(0001)$ crystal of 10 mm diameter and 1 mm thickness has been mounted on a custom built sapphire sample holder. The sapphire has a circular hole to expose the sample back for annealing by electron bombardment. To prevent beam damage a thin molybdenum sheet has been sandwiched between Ni_2P and sapphire covering the hole. The sample has then been degassed and cleaned by repeated cycles of 0.5 keV Argon sputtering for 20 min and annealing at 900 K for 1 h in ultra-high vacuum (UHV). After the initial cleaning procedure several preparations have been performed by sputtering (0.5 keV, 5 μA, Ar^+) followed by annealing of the sample at different temperatures in the range from 720 to 940 K. The pressure during annealing of the sample has been on the order of 10^{-7} Pa. Such treatments led to well ordered surfaces in STM and LEED imaging.

3. Results

The crystal structure of Ni_2P and its two inequivalent planar subunits (i.e., Ni_3P and Ni_3P_2 stoichiometry), which can be considered two possible (0001) surface terminations, are shown in Fig. 1. These two layers are stacked alternately along the [0001] direction to form the bulk crystal structure of Fe_2P type ($a = 0.59$ nm, $c = 0.34$ nm).[20,21] Although DFT calculations found a Ni_3P_2 surface termination to be thermodynamically slightly more stable than the Ni_3P termination,[14] both structures should be considered.[12,13,15] The bright spots appearing in the STM images have been assigned to P atoms and their p_z orbitals.[12,13,22] In those early works several superstructures have already been observed in addition to the (1 × 1) LEED pattern.[13]

In the present work we have observed a clear ($\sqrt{3} \times \sqrt{3}$) R30° LEED pattern after heating the $Ni_2P(0001)$ sample at more than 790 K as shown in Fig. 2. The corresponding

*E-mail address: askr@cat.hokudai.ac.jp

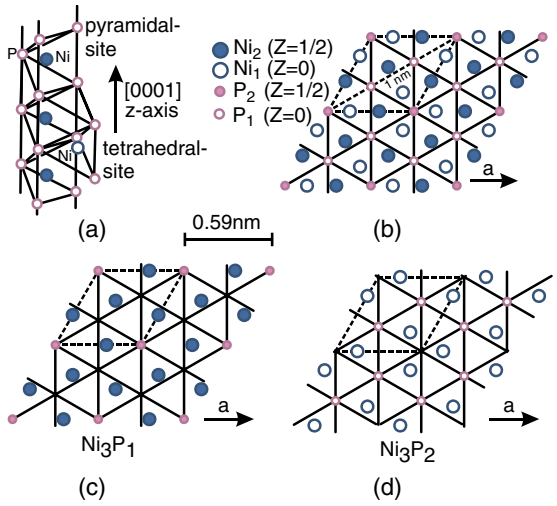

Fig. 1. (Color online) (a) Bulk crystal structure of Ni_2P (Fe_2P-type).[20] (b) Its projection along the [0001] direction. Inequivalent environments of two Ni and P sites are shown. (c) and (d) Top view of the two planar subunits of $Ni_2P(0001)$ with Ni_3P and Ni_3P_2 stoichiometry respectively. Each constitutes a possible bulk termination. Diamonds (dashed lines) enclose the projected bulk unit cell of $Ni_2P(0001)$.

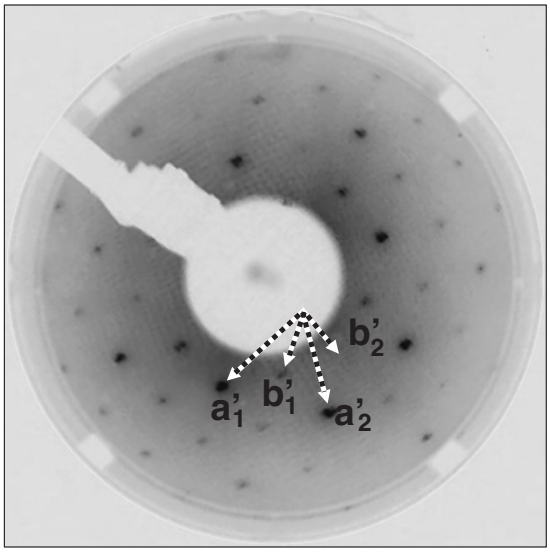

Fig. 2. (a) A LEED pattern of the $(\sqrt{3} \times \sqrt{3})$ R30° reconstruction observed at 73 eV beam energy. Bulk (a') and superstructure spots (b') are visible. Annealing temperature was 790 K during preparation.

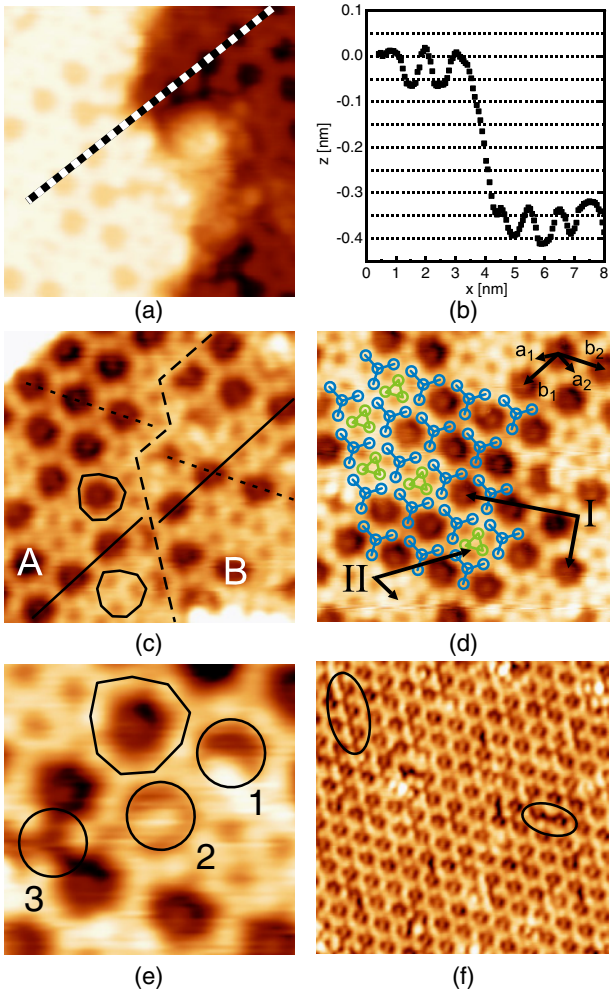

Fig. 3. (Color online) (a) STM image of a terrace step ($7 \times 7\,nm^2$, tunneling current $I_t = 10\,nA$ and sample bias $V_S = +40\,mV$). (b) Profile along the line indicated in (a). (c) Boundary (broken line) between two domains A and B of the superstructure. The lateral shift of rows of holes by about half a superstructure lattice constant perpendicular to the symmetry axes relative to the respective other domain is highlighted by dotted or solid lines ($6 \times 6\,nm^2$, $I_t = 5\,nA$, $V_S = +2\,mV$). (d) Atomic resolution STM image of empty (I) and filled (II) holes of the reconstruction. Propeller-like features and central triangles marked by circles and line segments ($7 \times 7\,nm^2$, $I_t = 10\,nA$, $V_S = -1\,mV$). (e) Local disorder in the reconstruction. Different added atoms in the empty holes (1) and (2) and a defect site (3) in the polygon framework ($3 \times 3\,nm^2$, $I_t = 10\,nA$, $V_S = -2\,mV$). (f) Completely empty structure after preparation at 940 K. Increased number of defects connects holes to short troughs marked by ellipses ($13 \times 13\,nm^2$, $I_t = 100\,pA$, $V_S = +50\,mV$).

STM images recorded from this superstructure are shown in Fig. 3. Terraces were found to be separated by steps of about 0.34 nm height matching the height of the bulk unit cell in the [0001] direction as shown in the line profile in Fig. 3(b). Domain boundaries such as indicated by a broken line in Fig. 3(c) are observed as well. There the superstructure is shifted laterally by about half its lattice constant perpendicular to its symmetry axes relative to the respective other domain as highlighted by dotted and solid lines. The STM images reveal a network composed of polygon-shaped units indicated by black lines in Figs. 3(c) and 3(e). Figure 3(d) shows a high resolution STM image. The separation between the units is 1.0 nm matching the long diagonal axis of the diamond shaped bulk surface cell as shown in Fig. 1. The units are oriented along $[30\bar{3}0]$ b_1 and $[\bar{3}300]$ b_2 directions. Thus, arrangement and dimensions of the units in STM and LEED patterns correspond well to a $(\sqrt{3} \times \sqrt{3})$ R30° structure. The large depressions of about 1 nm diameter occur as empty holes [marked by "I" in Fig. 3(d)] over the complete bias voltage range from below the Fermi level to +2.4 V. They are situated on the $(\sqrt{3} \times \sqrt{3})$ R30° reconstructed lattice. In other areas one finds the holes filled with bright spots [marked by "II" in Fig. 3(d)]. The framework around the holes is common to both structures. It consists of nine protrusions arranged in a polygon as highlighted with balls and sticks in Fig. 3(d). The polygon is composed of propeller-like structures and the central bright spots in "II" which form a triangle. The empty hole denoted as "I" has a

weak protrusion at the center as clearly visible in Fig. 3(d). The appearance of this weak protrusion changes with the tip condition and we tentatively assign it to be an artifact introduced by the tip probably due to an atomically sharp micro-tip sitting on a rather blunt macroscopic tip.

Upon annealing at 940 K all holes have been found empty as shown in Fig. 3(f). This all empty hole-type structure occurs concurrently with increased P desorption during the preparation at 940 K. Hence the empty type is related to empty P sites. In some cases the filled and empty structures of the $(\sqrt{3} \times \sqrt{3})$ R30° reconstruction show point defects with added or missing atoms indicated by circles in Fig. 3(e). Missing sites frequently occur at the propeller-like features as illustrated in Fig. 3(e). The partially filled holes constitute intermediate stages between the limiting configurations I and II. In the nearly all empty hole type structure, some of the edge atoms were missing and two or three holes connected to short troughs. Additional brighter protrusions are also observed in the defected polygons.

4. Discussion

Atomically resolved STM images of the $Ni_2P(0001)$ surface have been obtained. Terrace step heights have been found to match the bulk value, but lateral structures different from the two possible bulk terminations have been found on the surface. The STM data show two local structures compatible with the $(\sqrt{3} \times \sqrt{3})$ R30° structure: one being a filled and the other an empty network of polygons. Polygons are composed of propeller-like features and contain additional three central positions in the filled case. The sputtering of the $Ni_2P(0001)$ surface preferentially removes P atoms while annealing replaces the loss by supplying P from the bulk.[11] The desorption of P could be observed during heating under UHV conditions above 740 K. It increases with temperature and shows a significant increase around 970 K. This progressive desorption of P with increasing temperature is accompanied by a growing number of empty holes in the STM results. Therefore the reconstruction seems to be related to the removal of P atoms from the surface during the preparation. Although it is still difficult to derive a real space model for the $(\sqrt{3} \times \sqrt{3})$ R30° structure, we present some possibilities for further discussion. In analogy to works on Ni_3Al one might assume that P appears bright in STM images of $Ni_2P(0001)$ and $Ni_2P(10\bar{1}0)$ surfaces.[12,13,22] This can be rationalized by the large contribution of P p_z orbitals near the Fermi level similar to Ni_3Al surfaces, where the corresponding Al orbitals have been claimed to be responsible for the contrast,[23] although there is a local density of d states localized preferentially on Ni near the Fermi energy.[15,23] Therefore, we tentatively assign the bright spots to surface P atoms. By comparison of the bright spots with the atomic P positions in the $Ni_2P(0001)$ layers one finds three different sites. One can be assigned to the P position from the Ni_3P_2 structure and the other one to that from the Ni_3P structure. The third one has no corresponding P position in those two layers, but is thought to be a phosphorus atom that relaxed into the Ni site in the Ni_3P layer as shown in Fig. 4. The last two appear in the zone running along the b_2-direction, corresponding to the one unit vector direction of the

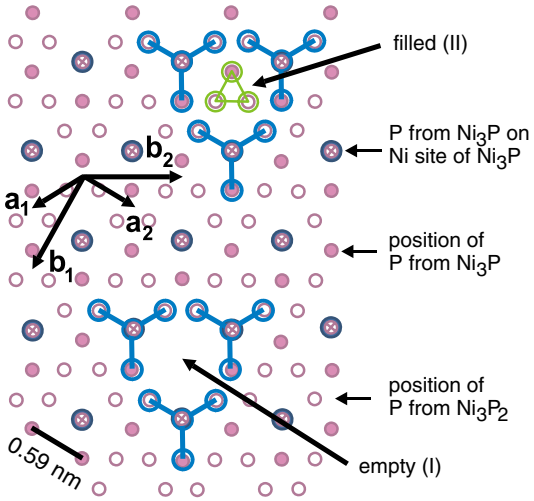

Fig. 4. (Color online) Proposed P positions for $(\sqrt{3} \times \sqrt{3})$ R30° structure based on the assumption that P is imaged in STM. Ni positions are not revealed and only proposed P positions are drawn. The structure emerges from the topmost Ni_3P and Ni_3P_2 layers. Ni sites of the Ni_3P layer get occupied by dislocated P.

$(\sqrt{3} \times \sqrt{3})$ R30° structure. In this zone two P atoms of Ni_3P_2 are missing. The P deficiency may induce the surface reconstruction including the reconstruction of Ni atoms. We are now carrying out further characterization like intensity-voltage (IV) LEED analysis to further evaluate the model structure.

5. Conclusions

In this paper we report STM results on a new reconstruction on the $Ni_2P(0001)$ surface. Data on dimensions, orientation and domain boundaries of the structure obtained with STM and LEED point to a $(\sqrt{3} \times \sqrt{3})$ R30° superstructure. The structure is composed of a framework of polygons formed by propeller-like arrangements of bright features as observed by STM. Polygons do or do not contain a triangle of positions in their center. With increasing annealing temperature during preparation the center triangle progressively vanishes. This corresponds to increasing P desorption with rising temperature during preparation. Finally the sole framework is left when preparation is performed at 970 K. The bright protrusions are tentatively interpreted as phosphorous on the basis of our experiences with the (1 × 1) surfaces of $Ni_2P(0001)$ and $Ni_2P(10\bar{1}0)$ and also in analogy to other intermetallic surfaces. Further accurate data in particular on surface stoichiometry, local environment of the individual species and electronic structure are necessary to develop a final model from these basic results.

Acknowledgments

This work is supported by a Grant-in-Aid for Scientific Research Category S (No. 16106010) from the Japan Society for the Promotion of Science, and Core Research for Evolutional Science and Technology from the Japan Science and Technology Agency. One of the authors (K.K.) is supported by a CRC international exchange program. The project is supported by GCOE "Catalyst Driven Innovation".

1) W. R. A. M. Robinson, J. N. M. van Gastel, T. I. Korányi, S. Eijsbouts, A. M. van der Kraan, J. A. R. van Veen, V. H., and J. de Beer: J. Catal. **161** (1996) 539.
2) T. I. Korányi: Appl. Catal. A **239** (2003) 253.
3) W. Li, B. Dhandapani, and S. T. Oyama: Chem. Lett. **27** (1998) 207.
4) C. Stinner, R. Prins, and Th. Weber: J. Catal. **191** (2000) 438.
5) C. Stinner, R. Prins, and Th. Weber: J. Catal. **202** (2001) 187.
6) P. Clark, W. Li, and S. T. Oyama: J. Catal. **200** (2001) 140.
7) S. T. Oyama, P. Clark, V. L. S. Teixiera da Silva, E. J. Lede, and F. G. Requejo: J. Phys. Chem. B **105** (2001) 4961.
8) C. Stinner, Z. Tang, M. Haouas, Th. Weber, and R. Prins: J. Catal. **208** (2002) 456.
9) S. T. Oyama, P. Clark, X. Wang, T. Shido, Y. Iwasawa, S. Hayashi, J. M. Ramallo-Lopez, and F. G. Requejo: J. Phys. Chem. B **106** (2002) 1913.
10) S. T. Oyama: J. Catal. **216** (2003) 343.
11) D. Kanama, S. T. Oyama, S. Otani, and D. F. Cox: Surf. Sci. **552** (2004) 8.
12) M. G. Moula, S. Suzuki, W.-J. Chun, S. Otani, S. T. Oyama, and K. Asakura: Chem. Lett. **35** (2006) 90.
13) M. G. Moula, S. Suzuki, W.-J. Chun, S. Otani, S. T. Oyama, and K. Asakura: Surf. Interface Anal. **38** (2006) 1611.
14) P. Liu, J. A. Rodriguez, T. Asakura, J. Gomes, and K. Nakamura: J. Phys. Chem. B **109** (2005) 4575.
15) Q. Li and X. Hu: Phys. Rev. B **74** (2006) 035414.
16) *Binary Alloy Phase Diagrams*, ed. T. B. Massalski, H. Okamoto, P. R. Subramanian, and L. Kacprzak (AMS International, Materials Park, OH, 1992) 2nd ed., Vol. 3.
17) O. N. Ilnitskaya, L. G. Akselrud, S. I. Mikhalenko, and Y. B. Kuzma: Kristallografiya **32** (1987) 50 [in Russian].
18) M. Heyde, M. Kulawik, H.-P. Rust, and H.-J. Freund: Rev. Sci. Instrum. **75** (2004) 2446.
19) H.-P. Rust, M. Heyde, and H.-J. Freund: Rev. Sci. Instrum. **77** (2006) 043710.
20) R. Fruchart, A. Roger, and J. P. Senateur: J. Appl. Phys. **40** (1969) 1250.
21) S. Rundqvist: Acta Chem. Scand. **16** (1962) 992.
22) S. Suzuki, M. G. Moula, Y. Nakagawa, K. Kinoshita, T. Miyamoto, K. Asakura, S. T. Oyama, and S. Otani: to be published in J. Nanosci. Nanotechnol.
23) L. Jurczyszyn, A. Rosenhahn, J. Schneider, C. Becker, and K. Wandelt: Phys. Rev. B **68** (2003) 115425.